Adsorption of Water Dimer on Platinum(111): Identification of the —OH···Pt Hydrogen Bond

Kenta Motobayashi,[*,†,‡,§] Líney Árnadóttir,[*,⊥,∥] Chikako Matsumoto,[§,#] Eric M. Stuve,[⊥] Hannes Jónsson,[▽] Yousoo Kim,[§] and Maki Kawai[*,‡]

[†]Catalysis Research Center, Hokkaido University, Sapporo 001-0021, Japan, [‡]Department of Advanced Materials Science, The University of Tokyo, Kashiwa 277-8561, Japan, [§]Surface and Interface Science Lab, RIKEN, Wako 351-0198, Japan, [⊥]Department of Chemical Engineering, Box 351750, University of Washington, Seattle, Washington 98195-1750, United States, [∥]School of Chemical, Biological and Environmental Engineering, Oregon State University, Corvallis, Oregon 97331, United States, [#]Department of Physics, Gakushuin University, Tokyo 171-8588, Japan, and [▽]Faculty of Physical Sciences, VR-III, University of Iceland, 107 Reykjavík, Iceland

ABSTRACT The fundamental structure of an isolated water dimer on Pt(111) was determined by means of a spectroscopic method using scanning tunneling microscopy (STM) and density functional theory (DFT) calculations. Two water molecules on adjacent atop sites form a dimer through a hydrogen bond, and they rotate even at a substrate temperature of 5 K. Action spectroscopy using STM (STM-AS) for water dimer hopping allows us to obtain the vibrational spectrum of a single water dimer on Pt(111). Comparisons between the experiments and theory show that one of the OH groups of the acceptor water molecule points toward the surface to form an —OH···Pt hydrogen bond.

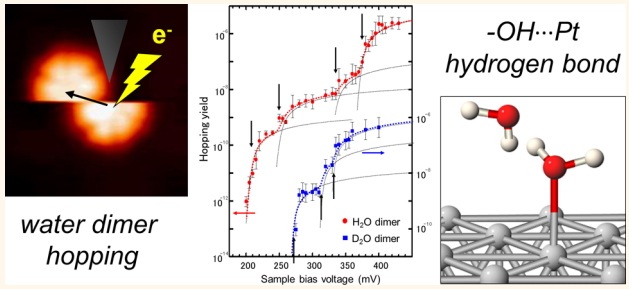

KEYWORDS: scanning tunneling microscopy · vibrational spectroscopy · water · DFT · surface science · hydrogen bond

Water adsorption on well-defined metal surfaces is a useful model system for exploring the nature of the hydrogen bond and hydrogen bonded networks at the molecular level. These play crucial roles in electrochemistry, heterogeneous catalysis, and various other fields of science.[1−7] The close-packed surfaces of single crystals of late transition metals (Pt, Pd, Ru, *etc.*) are often used as templates for growing two-dimensional water overlayers[8−14] and three-dimensional ice films[15−20] because the lattice constants of these surfaces match well with the intermolecular distances in ice. In particular, the structure of water overlayers on single-crystalline metal surfaces has been discussed as an important system for understanding water—water and water—metal interactions. In the early stages of this field of research, the ice "bilayer" model, in which water is only slightly distorted from its bulk ice arrangement,[21] was used to describe the water overlayer structure. Later, the difference between this simple model and the actual structure was determined to be too large, revealing that this model is inadequate.[5] Various studies sought to answer the following questions,[1−7] with controversial results because of the experimental difficulties in detecting complicated and fragile water overlayer structures: Does intact or dissociative adsorption occur? In which direction are the free OH groups oriented? Are water molecular networks commensurate with the substrate lattices?

The structures of water overlayers vary depending on the metal substrate, indicating that both structure and stability of the overlayers are governed by a subtle balance between water—water and water—metal interactions.[1−7] Regarding the overlayer on Pt(111), which is important because of its catalytic and electrocatalytic activity, a consensus has finally been reached: water molecules adsorb intact,[22] with an OH group pointing toward the metal surface (H-down structure),[23−26] forming slightly incommensurate overlayers with $(\sqrt{37} \times \sqrt{37})$ or $(\sqrt{39} \times \sqrt{39})$ structures.[13−16,27−29]

* Address correspondence to kmotobayashi@cat.hokudai.ac.jp, liney.arnadottir@oregonstate.edu, maki@k.u-tokyo.ac.jp.

Received for review August 27, 2014 and accepted October 22, 2014.

Published online October 22, 2014
10.1021/nn504824z

The structure of monomeric and small clusters of water on metal surfaces has attracted much attention and has been discussed extensively for its importance as a building block of water clusters and overlayers.[7,30−35] Among previously investigated water clusters, a water dimer on Pt(111)[24,29,36−39] is a simple system that is suitable for studies of the water−water and water−metal interactions. Its structure, especially the orientation of the OH groups that determine the water−metal interaction regime, is still debated, however. Studies using density functional theory (DFT) calculations of water dimers on Pt(111) have given different optimized structures.[29,37−39] Thus, experimental evidence is required to determine the structure. Monomeric or small clusters of water on Pt(111) have been studied with various experimental techniques, such as infrared reflection absorption spectroscopy (IRAS),[24,25,40] high-resolution electron energy loss spectroscopy (HREELS),[41,42] and helium-atom scattering.[43] These macroscopic vibrational spectroscopies probe an ensemble of water clusters, however, and the wide range of cluster sizes makes assignment of specific vibrational signals difficult.

In contrast to conventional macroscopic vibrational spectroscopy, scanning tunneling microscopy (STM) can be used to visualize molecules in real space and directly reveal the size of individual clusters.[30−35] Furthermore, STM enables the acquisition of vibrational spectra of single molecules and clusters through the use of inelastic electron tunneling spectroscopy (STM-IETS)[44] and action spectroscopy (STM-AS).[45] Therefore, STM can provide cluster-size-specific vibrational spectra of a monomer and clusters of water molecules on surfaces. The vibrational spectra can be used to determine the detailed structure of isolated molecules and clusters, including the orientation of the OH groups, providing insights into the dependence of molecule−metal and molecule−molecule interactions on cluster size. In STM-IETS, a small conductance change of the molecule due to the onset of inelastic electron tunneling is measured. This method is applicable to stable molecules on surfaces. In STM-AS, the increase in yields of the motion/reactions, induced by vibrational excitation due to inelastic electron tunneling, are monitored. This feature makes STM-AS the most suitable technique for obtaining cluster-size-specific vibrational spectra of water molecules, which have high diffusion rates even at low substrate temperatures (one exception is immobile water at elbow sites of the herringbone reconstruction of Au(111)[46]).

Recently, we developed a spectral fitting analysis method for STM-AS to enhance its performance and versatility.[47−49] The use of STM-AS originally suffered from scarcity of data points and was sensitive to errors in individual data points, which easily lead to artifacts. The vibrational energy was empirically determined by gradually increasing yields of the motions and reactions detected as a function of the sample bias voltage. Spectral fitting permits discrimination of vibrational signals from artifacts because of the strong vibrational energy dependence of the overall curve shape of the simulated spectra. Thus, spectral fitting provides evidence for determining the vibrational energy from the spectral shape, which enhances the "apparent" energy resolution. This powerful technique is well suited for determining the detailed structure of a water dimer on Pt(111).

In this letter, we present a combined STM and DFT study of the structure of a water dimer adsorbed on Pt(111). The STM observations revealed that both water molecules in the dimer are adsorbed on atop sites and that one of the water molecules can rotate around the other, even at a substrate temperature of 5 K. Using STM-AS, we obtained the vibrational spectrum of a single water dimer. A comparison of the experimentally and theoretically obtained vibrational spectra made it possible to determine the detailed structure of the adsorbed dimer, revealing that one of the OH groups points toward the surface to form an −OH···Pt hydrogen bond.

RESULTS AND DISCUSSION

At low coverage (<0.005 ML), monomers and dimers were observed as round- and "flower"-shaped protrusions, respectively, in the STM images (Figure 1a−c).[36] Both H_2O and D_2O resulted in identical protrusions. The assignment of monomers and dimers is based on the manipulation experiment. The collision of two round protrusions (Figure 1d), which was induced by applying a voltage pulse (typically 200 mV, 1 nA, 1 s) to one protrusion (Figure 1e), resulted in a flower-shaped protrusion (Figure 1f).

The water monomer's center of mass resides on the atop site, which was determined from the atomically resolved STM image taken with a molecular tip (a water molecule is attached on the apex of the tip), as shown in Figure 1b. This STM image supports results of the DFT calculation indicating that monomers adsorb on atop sites with their molecular plane parallel to the metal substrate.[29,38,50] In addition, DFT studies indicated that the lateral rotation barriers of water monomers are very low and that they can rotate freely at a finite temperature.[38,50] Thus, the monomers are imaged as circular protrusions in STM.

The atomically resolved STM image of a water dimer shows that the center of mass of the dimer and the center of each lobe are all located on atop sites, as depicted in Figure 1c. The anomalous shape of the water dimer can be explained as a "time-averaged" 6-fold shape resulting from the rotation of one molecule around the other molecule fixed on the surface. This interpretation agrees with previous reports of rotating molecules (CO dimers[51] and CH_3SH monomers[52] on Au(111) at 5 K, and 2,5-dichlorothiophenol on Cu(111) at

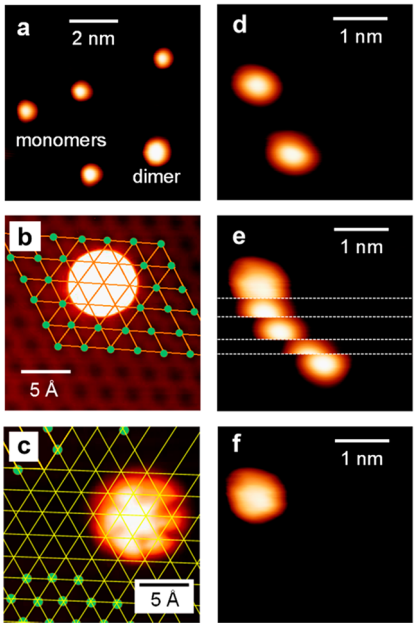

Figure 1. STM images of (a) H_2O monomers and a dimer on Pt(111) (sample bias voltage V_s = 50 mV and tunneling current I_t = 1.0 nA); (b) a H_2O monomer taken with a tip on which a water molecule was attached to the apex (molecular tip) to resolve the Pt lattice; the grid shows the positions of the Pt atoms (V_s = 20 mV, I_t = 0.5 nA); (c) a H_2O dimer taken with a molecular tip (V_s = 20 mV, I_t = 0.5 nA); (d) H_2O monomers (V_s = 50 mV, I_t = 0.8 nA); (e) the manipulation of a H_2O monomer to bind with another H_2O monomer to form a dimer (V_s = 50 mV, I_t = 0.8 nA); and (f) the H_2O dimer formed in the manipulation experiment (V_s = 50 mV, I_t = 0.8 nA). In (e), when the STM tip reached each white broken line during upward scanning, the STM tip was moved to the top of the monomer, a voltage pulse was applied (200 mV, 1 nA, 1 s), and scanning was resumed from the white line.

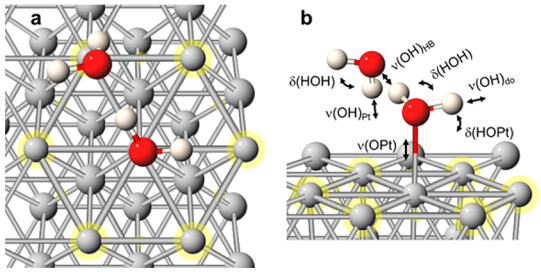

Figure 2. A top view (a) and a three-quarter view (b) of the optimized structure of a water dimer on Pt(111) based on the DFT calculations. The six Pt atoms that are above the potential minima for the H-acceptor molecule are highlighted. The notation of vibrational modes detected in the present study are indicated in (b).

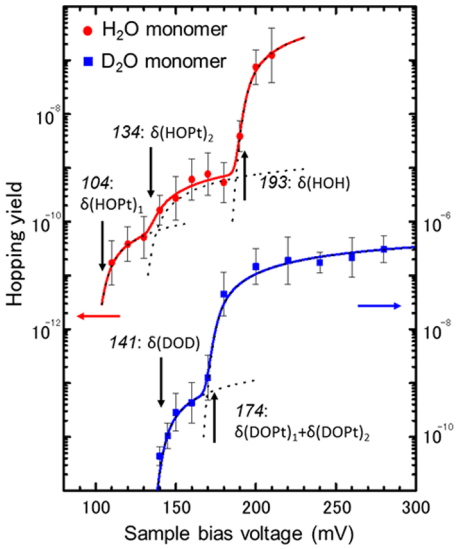

Figure 3. STM-AS and spectral fit of the lateral hopping of H_2O and D_2O monomers on Pt(111). The red circles and blue squares represent the experimental results of STM-AS for H_2O and D_2O, respectively. The thick solid curves represent the best-fit spectra, and the broken curves represent the fraction of simulated $Y(V)_{tot}$. The Ω determined by these fits are indicated with arrows in units of meV.

15 K).[53] Six equivalent potential minima for the rotating molecules at six atop sites resulted in a flower-shaped protrusion. In addition, the adsorption structure model of the water dimer is supported by the DFT calculations. In the optimized structure of a water dimer on Pt(111) (depicted in Figure 2), both water molecules are located at atop sites. The molecule that serves as a hydrogen-bond donor (H-donor molecule) is located near the surface and forms a stronger bond with an underlying Pt atom than does the hydrogen-bond acceptor molecule (H-acceptor molecule). Other DFT calculations[29,38,50] also show adsorption of both molecules at atop sites.

Because the dimer shows a flower-shaped protrusion regardless of the scanning conditions (2−100 mV, 0.05−10 nA), neither the tunneling current nor the applied electric field cause rotation of the water dimer. The potential-energy barrier for rotation of the H-acceptor molecule was calculated by DFT to be ∼20 meV.[38] The vibrational energy of the hindered lateral rotational mode of the H-acceptor molecule was calculated to be 42 meV. According to the harmonic approximation, the zero-point energy of this vibrational mode would be half of its vibrational energy, 21 meV, which is slightly higher than the barrier of rotation. Thus, we conclude that the zero-point energy of the hindered rotational mode allows the H-acceptor molecule to rotate around the H-donor molecule. The small energy barrier for the rotation suggests a small difference in energy for adsorption sites near the atop sites for H-acceptor molecules. This small difference contributes to the stability of the incommensurate ($\sqrt{37} \times \sqrt{37}$) and ($\sqrt{39} \times \sqrt{39}$) structures,[13−16,27−29] where the adsorption sites of some molecules are slightly shifted from the atop sites.

The water monomer hopping induced by inelastic electron tunneling (as shown in Figure 1e) was studied in further detail. Figure 3 shows the STM-AS, that is, the sample bias dependence of the yield of the lateral hopping of H_2O and D_2O monomers. The lateral hopping yield is determined from the tunneling current, and the time required for the molecule to hop that

appears in the $I-t$ plot as a result of tunneling electrons injected from the STM tip fixed above the center of a molecule, as described in the Methods section in more detail. At a glance, we defined threshold voltages of ~100 and ~200 mV for H_2O and ~140 and ~170 mV for D_2O. We applied spectral fitting analyses using eq 1, which is described in the Methods section, and identified five vibrational signals corresponding to δ(HOH), δ(DOD), two types of δ(HOPt), and a combination of two δ(DOPt). The resulting parameters are listed in Table 1. The vibrational energies obtained by STM-AS match well with those obtained by the DFT calculations of Meng *et al.* The water monomers begin to hop at ~100 mV. We confirmed that this hopping is a one-electron process on the basis of the nearly constant reaction yield at different tunneling currents and the fitting parameters of $n = 1$ for all the observed vibrational signals determined by the spectral fit (Table 1). Thus, the diffusion barrier of a water monomer is lower than 100 meV.

TABLE 1. Best-Fit Parameters for the Spectral Fitting of STM-AS for a Water Monomer on Pt(111)

assignment	Ω (meV)	n	$-\log K$	γ (meV)	Ω_{ref} (meV)[a]
$\delta(HOPt)_1$	104 ± 5	1	9.6	5	113
$\delta(HOPt)_2$	134 ± 5	1	8.6	5	121
$\delta(HOH)$	192 ± 2	1	5.8	5	190
$\delta(DOD)$	141 ± 2	1	8.4	5	141[b]
$\delta(DOPt)_1 + \delta(DOPt)_2$	174 ± 2	1	6.1	5	177 (77 + 100)[b]

[a] Ref 34. [b] Vibrational energies of D_2O were obtained using the values for H_2O and an isotope factor of 1.35.

As shown in Figure 4a–c, lateral hopping of the H_2O and D_2O dimers was observed when the STM tip was placed above the center of the dimer and a voltage pulse was applied (typically 250 mV, 1 nA, 1 s for H_2O dimer). We measured the STM-AS of the lateral hopping to obtain vibrational spectra and to characterize the hopping of single water dimers. Hopping of the water dimer was detected as a sudden current change in the $I-t$ plot (Figure 4c) and was confirmed by STM imaging (Figure 4a,b). Figure 4d is the STM-AS of the H_2O and D_2O dimers; *i.e.*, the lateral hopping yield as a function of sample bias voltage. At a glance, we defined several threshold voltages for the positive bias region, including ~200 and ~360 mV for H_2O and ~270, ~320, and ~340 mV for D_2O as previously reported.[36]

Water dimers rarely hop when δ(HOPt) at ~130 meV is excited and begin hopping at $V >$ ~200 mV. We confirmed that the hopping of water dimers is also a one-electron process as in the case of the monomer. These results indicate that the diffusion barrier E_B for water dimer is $130 < E_B < 200$ meV. Dimers on Pt(111) should have a higher diffusion barrier and greater stability than those of monomers on Pt(111). The

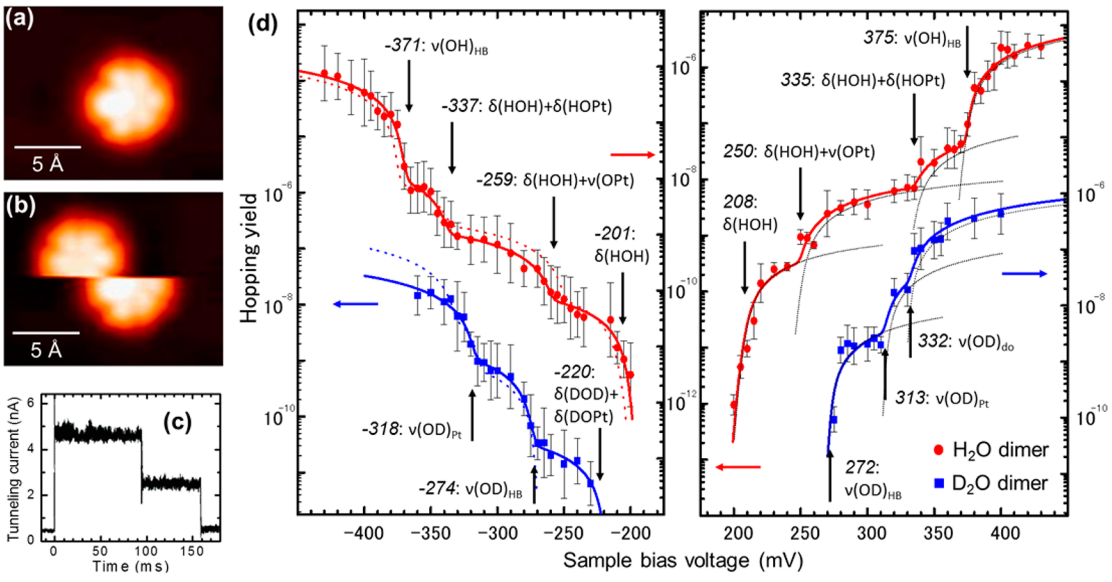

Figure 4. (a) STM image of a H_2O dimer on Pt(111) ($V_s = 40$ mV, $I_t = 1.0$ nA). (b) STM image of the H_2O dimer before and after lateral hopping was induced ($V_s = 40$ mV, $I_t = 1.0$ nA). The STM tip was scanned from the bottom to the middle of the figure and was then positioned on top of the water dimer. A voltage pulse (250 mV, 5 nA, 1 s) was applied before the scan was restarted from the middle to the top of the image. (c) The tunneling current measured as a function of time under constant applied voltage (280 mV, 4.5 nA, 160 ms). (d) STM-AS and spectral fit of the lateral hopping of H_2O and D_2O dimers on Pt(111) at positive (right) and negative (left) sample bias voltages. The red circles and blue squares represent the experimental results of the STM-AS for H_2O and D_2O, respectively. In the previous report, error bars were calculated for positive bias before the logarithm of $Y(V)$ was taken.[36] Here, error bars of logarithmic $Y(V)$ are plotted. The thick solid curves represent the best-fit spectra. The thin dotted curves at positive bias represent the fraction of simulated $Y(V)_{tot}$, representing the $Y(V)$ of hopping induced by the excitation of each vibrational mode. The broken curves at negative bias are simulated hopping yield at negative bias $Y(V)_{neg}$ shown for comparison, which were obtained by $Y(V)_{neg} = 0.2Y(-V)_{pos}$, where $Y(V)_{pos}$ is $Y(V)$ obtained by spectral fit at positive bias. The Ω values determined by this fit are indicated by arrows (in units of meV).

TABLE 2. Best-Fit Parameters for the Spectral Fitting of STM-AS at Positive Sample Bias Voltage and Calculated Vibrational Energies for a Water Dimer on Pt(111)[a]

assignment	Ω (meV)	*n*	−log *K*	γ (meV)	Ω_{down} (meV)	Ω_{para} (meV)
δ(HOH)	208 ± 6 (−201 ± 6)	1	8.7 (9.5)	5	198, 193	198
δ(HOH) + ν(OPt)	250 ± 6 (−259 ± 6)	1	7.6 (8.4)	5	244 (198 + 46)	242 (198 + 44)
δ(HOH) + δ(HOPt)	335 ± 5 (−337 ± 6)	1	6.5 (7.1)	5	329 (198 + 131)	331 (198 + 133)
$\nu(OH)_{HB}$	375 ± 3 (−371 ± 6)	1	4.7 (5.3)	5	362	347
$\nu(OD)_{HB}$	272 ± 3 (−274 ± 6)	1	7.6 (8.1)	5	264	257[b]
$\nu(OD)_{Pt}$	313 ± 3 (−318 ± 6)	1	6.4 (6.8)	5	309	320[b]
$\nu(OD)_{do}$	332 ± 3	1	5.6	5	336	335[b]

[a] The values in parentheses for Ω and −log *K* represent the best-fit parameters for the spectra at negative bias. The Ω_{down} values represent the theoretically obtained results in this study, and the Ω_{para} values are from ref 34. [b] Vibrational energies of D_2O were obtained using those of H_2O from ref 34 and an isotope factor of 1.35. δ: libration, ν: stretching.

diffusion barriers of water on Pt(111) based on DFT calculations follow this trend.[39] However, this tendency is the opposite on Pd(111), where instantaneous diffusion of a dimer and stable monomers was reported at 40 K.[31] This difference is probably due to a different diffusion mechanism of water dimers on Pt(111) and Pd(111), such as tunneling-exchange-assisted diffusion.[54]

Application of a theoretical fit[47] to the spectra makes it possible to extract more information from the STM-AS data on the water dimer. The experimental results are well represented by the simulated curves (thick solid curves in Figure 4d) with vibrational signals in the positive bias region at 208, 250, 335, and 375 meV for H_2O and at 272, 313, and 332 meV for D_2O. The best-fit parameters are listed in Table 2. Because eq 1 (given in the Methods section) represents the spectral shape of *Y*(*V*) not only near the vibrational energy of the corresponding mode but also over a wide range of *V*, the results are not significantly affected by the experimental errors of each data point. Thus, we can reasonably assign the yield increase at ∼250 and ∼335 mV for H_2O to the vibrational signals.

DFT calculations of the vibrational frequencies of both H_2O and D_2O dimers on Pt(111) allow assignment of the vibrational signals observed in the STM-AS, as summarized in Table 2. A comparison of the values for Ω_{down} obtained in this study indicates that the signal at 208 meV corresponds to the HOH scissoring modes δ(HOH) of H-donor and H-acceptor molecules which overlap each other. The small signals at 250 and 335 meV are, respectively, the combination modes of the δ(HOH) and O−Pt stretching modes of the H-donor molecule ν(OPt), and of the δ(HOH) and libration modes of the H−O−Pt of the H-donor molecule δ(HOPt). The signal at 375 mV represents the OH stretching mode of the H-donor molecule, which participates in an intermolecular hydrogen bond $\nu(OH)_{HB}$. The signals for D_2O at 272, 313, and 332 meV respectively correspond to $\nu(OD)_{HB}$, the OD stretching mode of the H-acceptor molecule that points toward the surface $\nu(OD)_{Pt}$, and the free OD stretching mode of the H-donor ($\nu(OD)_{do}$).

We measured the STM-AS at both positive and negative sample bias voltages to confirm that the observed signals resulted from vibrational excitations. Consequently, we obtained similar spectra with slightly smaller *Y*(*V*) or *K* values, and nearly equal vibrational energies and other parameters, except for $\nu(OD)_{do}$ (as shown in Figure 4d and Table 2). The $Y(V)_{neg}$, hopping yield at negative bias obtained by $Y(V)_{neg} = 0.2Y(-V)_{pos}$ (the broken curves in Figure 4d at negative bias) where $Y(V)_{pos}$ is obtained by spectral fit at positive bias (the solid curves at positive bias), approximately represents the experimental results at negative bias. The small signals at 250 and 335 mV appear in both spectra, indicating that these signals did not result from differences in the electronic density of states (DOS) or from artifacts caused by errors but rather from the vibrational excitation of the combination modes.

Such linear relationships between spectra at positive and negative sample bias voltages have been reported[49,55] and explained on the basis of the resonant model for vibrational excitation through inelastic electron tunneling.[56] In this model, an incident electron is temporarily captured by a molecular orbital (MO) localized in a resonant state, resulting in the excitation of molecular vibrations. Therefore, the vibrational excitation probability depends on the electronic DOS of the responsible MO that is localized below the STM tip at corresponding energies. Among the parameters used in the spectral fitting, only *K* is affected by the electronic DOS; therefore, this difference in electronic DOS potentially resulted in slightly different *Y*(*V*) or *K* values for a water dimer with similar overall spectral features at positive and negative sample biases. We believe that the absence of $\nu(OD)_{do}$ at a negative sample bias is also due to the difference in populations and the spatial distributions of the MOs at positive and negative biases.

A vibrational signal corresponding to $\nu(OH)_{HB}$ at 375 mV in the STM-AS of the H_2O dimer was observed in the IRAS of H_2O on Pt(111) for large islands in which the OH groups are located at the edge of the island and point toward the surface at 40 K.[25] This $\nu(OH)_{HB}$, with an energy value of approximately 375 mV, was absent

in previously reported IRAS[24,25] and HREELS[42] spectra for low H_2O coverage. Nakamura *et al.* attributed the vibrational signals in IRAS to water monomers, dimers, and tetramers,[24] whereas Ogasawara *et al.* assigned them to only monomers and dimers.[25] The vibrational features of the water dimers observed here by STM-AS suggest that water dimers were not observed in these macroscopic vibrational studies. We believe that, at a coverage of 0.07−0.09 ML as was used in the IRAS experiments, clusters larger than dimers are mainly formed and detected. Thus, STM-AS appears to be the only method so far that can detect the vibrational signals of water dimers on metal surfaces.

The vibrational energy of ν(OH(D)) can be used to deduce the structure of water dimers because it depends on the environment surrounding each OH(D) group. Meng *et al.* reported a DFT calculation of the water dimer structure in which the H-acceptor molecule has two OH(D) groups that are equivalently oriented toward the surface (H-parallel model).[29,37] In addition, another structure model has been reported in which one OH(D) of the H-acceptor molecule points toward the surface and the other points toward the vacuum (H-down model).[38] To determine which structure occurred in our experiment, we compared the measured vibrational energies with the calculated vibrational energies of the H-parallel and H-down models (Ω_{para} and Ω_{down}), as shown in Table 2. The vibrational energies obtained by STM-AS show better agreement with the vibrational energies calculated for the H-down model, Ω_{down}. The vibrational energy of the H-parallel model shows significant disagreement, especially in $\nu(OH(D))_{HB}$. Thus, we conclude that the water dimer structure on Pt(111) observed in our STM measurements is well represented by the H-down model. Consequently, the regime of the water−metal interaction is also suggested. The H-donor molecule interacts with the substrate Pt atoms *via* back-donation of the oxygen lone pair as commonly thought.[29,37] The H-acceptor molecule interacts with the Pt substrate not through the oxygen lone pair as suggested in the H-parallel model[29,37] but through an −OH···Pt hydrogen bond.

By applying spectral fitting to the STM-AS data and comparing the fits with the DFT calculations, we have been able to determine the positions of the H(D) atoms in individual molecules, which is a difficult task even when using STM. This provides valuable information regarding a long-discussed issue of the interaction regimes between the H-acceptor molecule and the substrate, in particular the possibility of an −OH···Pt hydrogen bond. Vibrational signals of $\nu(OH(D))_{HB}$ indicating similar H-down structure were observed at the edges of larger clusters.[25,57] The similar H-down structures of the water dimer and cluster edge suggested that the dangling OH pointing toward the vacuum is less stable and is more likely to interact with the Pt substrate. In contrast, this vibrational signal is absent for the H-down structure of the water overlayers,[25] suggesting that the hydrogen bonding network between the water molecules alters the bonding regime between the water molecules and the metal substrates.

CONCLUSIONS

In this study, STM-AS experiments with spectral fitting, in conjunction with DFT calculations, were used to determine the detailed structure and the interaction regime of a water dimer adsorbed on Pt(111). The STM-AS measurements with spectral fitting revealed most of the normal vibrational modes and some combination modes of a water dimer. By comparing the experimentally observed vibrational energies with those obtained by DFT calculations, we determined the structure of the water dimer adsorbed on Pt(111), where one OH(D) group of the hydrogen-bond acceptor molecule points toward the surface to form an −OH···Pt hydrogen bond. We demonstrated that the STM-AS with improved apparent energy resolution due to spectral fitting enables us to determine the internal structure of a single molecular cluster adsorbed on a surface.

Comparative studies on other metal substrates using STM-AS would contribute to a deeper and more general understanding regarding the balance between water−water and water−metal interactions and could also shed light on the origin of the differences observed in the water bilayer structures on various metal surfaces. We believe that the H-down structure of the water dimer found here may provide important information for various chemistry-related investigations. One example relates to hydrogen production *via* the electrolysis of water at the surface of a metal electrode, an important process for energy storage.

METHODS

All of the experiments were performed using low-temperature STM (LT-STM, Omicron GmbH) equipped with an ultrahigh vacuum ($<3 \times 10^{-11}$ Torr) chamber. The single crystal surface of Pt(111) was prepared using cycles of Ar^+ ion sputtering and annealing at 1100 K. The Pt(111) surface was maintained at a temperature less than 20 K and exposed to a small amount of water molecules (H_2O or D_2O) through a dosing tube.[36] All of the STM measurements were performed at 5 K.

The STM-AS is a spectroscopic method capable of measuring the vibrational spectra of a single molecule. When tunneling electrons are injected into the target molecule at various sample biases V, the yield $Y(V)$ of vibrationally induced molecular motions or reactions remarkably increases at V that corresponds to the vibrational energy. Thus, systematic measurements of $Y(V)$ provide the vibrational features of the target molecule. Detailed information regarding the molecule was obtained using a spectral fitting analysis of STM-AS, as described below.

The hopping yields of the water monomers and dimers were measured as follows.[36,45,58] After an STM image was obtained, the STM tip was fixed over the center of a target molecule. Next, tunneling electrons were injected into the molecule at a certain constant sample bias voltage with the feedback loop off. We detected the hopping from sudden changes in the tunneling current in the $I-t$ plot and confirmed it using subsequent STM imaging, as shown in Figure 4c and b, respectively. The hopping yield Y was calculated from $Y = e/I\tau$, where e is the elementary charge and τ is the time required for hopping. The averaged values of $Y(V)$ were obtained by repeating the aforementioned experiment 16 times for each value of V.

The spectral fitting analysis of STM-AS is described elsewhere.[47−49,59,60] Because the second derivative of the tunneling current gives the vibrational density states (DOS) in the STM-IETS, the inelastic tunneling current responsible for motion and reactions of the target molecules was derived from double integration of a Gaussian function representing the vibrational DOS $\rho_{ph}(\omega)$. Because the reaction rate is proportional to the inelastic tunneling current and the yield is obtained by dividing the reaction rate by the total current, the total reaction yield $Y(V)_{tot}$ can be expressed as follows:

$$Y(V)_{tot} = \sum_i K_i \frac{f(V, \Omega_i, \gamma_i)^{n_i}}{V} \quad (1)$$

$$f(V, \Omega, \gamma) = \frac{1}{e}\int_0^{eV} d\omega \int_0^{\omega} \rho_{ph}(\omega')\, d\omega' \quad (2)$$

where i is an index of the vibrational signals, K is the rate constant, Ω is the vibrational energy, γ is a vibrational broadening factor, and n is the reaction order, which is equal to the number of electrons required for the reaction. Several parameters, such as the vibrational energies, were determined using a least-squares fit of eq 1 to the STM-AS experimental data.

The details of the DFT calculations have been described elsewhere.[38,39] Briefly, all of the calculations were performed using the Vienna ab initio simulation package (VASP)[61−64] and a plane-wave implementation of DFT using the PW91 functional.[65] The interactions between the ions and valence electrons were described by ultrasoft Vanderbilt pseudopotentials,[66,67] and a cutoff energy of 396 eV (29 Ry). The Brillouin zone was sampled using a $2 \times 2 \times 1$ Monkhorst−Pack k-point mesh. The optimized structure of the H_2O dimer on Pt(111)[38] was calculated using 36 substrate atoms, with 12 atoms per layer in three layers. The vibrational energies of both H_2O and D_2O dimers were calculated.

Conflict of Interest: The authors declare no competing financial interest.

Acknowledgment. This work is supported in part by a Grant-in-Aid for Scientific Research on Priority Areas "Electron Transport Through a Linked Molecule in Nano-scale" and a Grant-in-Aid for Scientific Research (S) "Single Molecule Spectroscopy using Probe Microscope" from the Ministry of Education, Culture, Sports, Science, and Technology (MEXT) of Japan. In addition, K.M. acknowledges the support of the JSPS (Japan Society for the Promotion of Science).

REFERENCES AND NOTES

1. Thiel, P. A.; Madey, T. E. The Interaction of Water with Solid Surfaces: Fundamental Aspects. *Surf. Sci. Rep.* **1987**, *7*, 211–385.
2. Henderson, M. A. The Interaction of Water with Solid Surfaces: Fundamental Aspects Revisited. *Surf. Sci. Rep.* **2002**, *46*, 1–308.
3. Verdaguer, A.; Sacha, G. M.; Bluhm, H.; Salmeron, M. Molecular Structure of Water at Interfaces: Wetting at the Nanometer Scale. *Chem. Rev.* **2006**, *106*, 1478–1510.
4. Michaelides, A. Density Functional Theory Simulations of Water−Metal Interfaces: Waltzing Waters, a Novel 2D Ice Phase, and More. *Appl. Phys. A: Mater. Sci. Process.* **2006**, *85*, 415–425.
5. Hodgson, A.; Haq, S. Water Adsorption and the Wetting of Metal Surfaces. *Surf. Sci. Rep.* **2009**, *64*, 381–451.
6. Carrasco, J.; Hodgson, A.; Michaelides, A. A Molecular Perspective of Water at Metal Interfaces. *Nat. Mater.* **2012**, *11*, 667–674.
7. Tatarkhanov, M.; Ogletree, D. F.; Rose, F.; Mitsui, T.; Fomin, E.; Maier, S.; Rose, M.; Cerdá Jorge, I.; Salmeron, M. Metal- and Hydrogen-Bonding Competition During Water Adsorption on Pd(111) and Ru(0001). *J. Am. Chem. Soc.* **2009**, *131*, 18425–18434.
8. Held, G.; Menzel, D. The Structure of the P($\sqrt{3} \times \sqrt{3}$)R30° Bilayer of D_2O on Ru(001). *Surf. Sci.* **1994**, *316*, 92–102.
9. Held, G.; Menzel, D. Structural Isotope Effect in Water Bilayers Adsorbed on Ru(001). *Phys. Rev. Lett.* **1995**, *74*, 4221.
10. Feibelman, P. J. Partial Dissociation of Water on Ru(0001). *Science* **2002**, *295*, 99–102.
11. Haq, S.; Clay, C.; Darling, G. R.; Zimbitas, G.; Hodgson, A. Growth of Intact Water Ice on Ru(0001) between 140 and 160 K: Experiment and Density-Functional Theory Calculations. *Phys. Rev. B: Condens. Matter Mater. Phys.* **2006**, *73*, 115414.
12. Michaelides, A.; Alavi, A.; King, D. A. Different Surface Chemistries of Water on Ru{0001}: From Monomer Adsorption to Partially Dissociated Bilayers. *J. Am. Chem. Soc.* **2003**, *125*, 2746–2755.
13. Nie, S.; Feibelman, P. J.; Bartelt, N. C.; Thürmer, K. Pentagons and Heptagons in the First Water Layer on Pt(111). *Phys. Rev. Lett.* **2010**, *105*, 026102.
14. Standop, S.; Redinger, A.; Morgenstern, M.; Michely, T.; Busse, C. Molecular Structure of the H_2O Wetting Layer on Pt(111). *Phys. Rev. B: Condens. Matter Mater. Phys.* **2010**, *82*, 161412.
15. Zimbitas, G.; Haq, S.; Hodgson, A. The Structure and Crystallization of Thin Water Films on Pt(111). *J. Chem. Phys.* **2005**, *123*, 174701.
16. Haq, S.; Harnett, J.; Hodgson, A. Growth of Thin Crystalline Ice Films on Pt(111). *Surf. Sci.* **2002**, *505*, 171–182.
17. Thürmer, K.; Bartelt, N. C. Nucleation-Limited Dewetting of Ice Films on Pt(111). *Phys. Rev. Lett.* **2008**, *100*, 186101.
18. Kondo, T.; Kato, H. S.; Bonn, M.; Kawai, M. Morphological Change During Crystallization of Thin Amorphous Solid Water Films on Ru(0001). *J. Chem. Phys.* **2007**, *126*, 131103.
19. Kondo, T.; Mae, S.; Kato, H. S.; Kawai, M. Morphological Change of D_2O Layers on Ru(0001) Probed with He Atom Scattering. *Surf. Sci.* **2006**, *600*, 3570–3574.
20. Haq, S.; Hodgson, A. Multilayer Growth and Wetting of Ru(0001). *J. Phys. Chem. C* **2007**, *111*, 5946–5953.
21. Doering, D. L.; Madey, T. E. The Adsorption of Water on Clean and Oxygen-Dosed Ru(011). *Surf. Sci.* **1982**, *123*, 305–337.
22. Fisher, G. B.; Gland, J. L. The Interaction of Water with the Pt(111) Surface. *Surf. Sci.* **1980**, *94*, 446–455.
23. Ogasawara, H.; Brena, B.; Nordlund, D.; Nyberg, M.; Pelmenschikov, A.; Pettersson, L. G. M.; Nilsson, A. Structure and Bonding of Water on Pt(111). *Phys. Rev. Lett.* **2002**, *89*, 276102.
24. Nakamura, M.; Shingaya, Y.; Ito, M. The Vibrational Spectra of Water Cluster Molecules on Pt(111) Surface at 20 K. *Chem. Phys. Lett.* **1999**, *309*, 123–128.
25. Ogasawara, H.; Yoshinobu, J.; Kawai, M. Clustering Behavior of Water (D_2O) on Pt(111). *J. Chem. Phys.* **1999**, *111*, 7003–7009.
26. Ogasawara, H.; Yoshinobu, J.; Kawai, M. Water Adsorption on Pt(111): From Isolated Molecule to Three-Dimensional Cluster. *Chem. Phys. Lett.* **1994**, *231*, 188–192.
27. Harnett, J.; Haq, S.; Hodgson, A. Electron Induced Restructuring of Crystalline Ice Adsorbed on Pt(111). *Surf. Sci.* **2003**, *528*, 15–19.
28. Feibelman, P. J.; Bartelt, N. C.; Nie, S.; Thürmer, K. Interpretation of High-Resolution Images of the Best-Bound Wetting Layers on Pt(111). *J. Chem. Phys.* **2010**, *133*, 154703.
29. Meng, S.; Wang, E. G.; Gao, S. Water Adsorption on Metal Surfaces: A General Picture from Density Functional

Theory Studies. *Phys. Rev. B: Condens. Matter Mater. Phys.* **2004**, *69*, 195404.
30. Morgenstern, K.; Rieder, K. H. Formation of the Cyclic Ice Hexamer *via* Excitation of Vibrational Molecular Modes by the Scanning Tunneling Microscope. *J. Chem. Phys.* **2002**, *116*, 5746–5752.
31. Mitsui, T.; Rose, M. K.; Fomin, E.; Ogletree, D. F.; Salmeron, M. Water Diffusion and Clustering on Pd(111). *Science* **2002**, *297*, 1850–1852.
32. Morgenstern, K.; Gawronski, H.; Mehlhorn, T.; Rieder, K. H. Local Investigation of Electron-Induced Processes in Water-Metal Systems. *J. Mod. Opt.* **2004**, *51*, 2813–2819.
33. Mugarza, A.; Shimizu, T. K.; Frank Ogletree, D.; Salmeron, M. Chemical Reactions of Water Molecules on Ru(0001) Induced by Selective Excitation of Vibrational Modes. *Surf. Sci.* **2009**, *603*, 2030–2036.
34. Michaelides, A.; Morgenstern, K. Ice Nanoclusters at Hydrophobic Metal Surfaces. *Nat. Mater.* **2007**, *6*, 597–601.
35. Morgenstern, K.; Nieminen, J. Intermolecular Bond Length of Ice on Ag(111). *Phys. Rev. Lett.* **2002**, *88*, 066102.
36. Motobayashi, K.; Matsumoto, C.; Kim, Y.; Kawai, M. Vibrational Study of Water Dimers on Pt(111) Using a Scanning Tunneling Microscope. *Surf. Sci.* **2008**, *602*, 3136–3139.
37. Meng, S.; Xu, L. F.; Wang, E. G.; Gao, S. Vibrational Recognition of Hydrogen-Bonded Water Networks on a Metal Surface. *Phys. Rev. Lett.* **2002**, *89*, 176104.
38. Árnadóttir, L.; Stuve, E. M.; Jónsson, H. Adsorption of Water Monomer and Clusters on Platinum(111) Terrace and Related Steps and Kinks I. Configurations, Energies, and Hydrogen Bonding. *Surf. Sci.* **2010**, *604*, 1978–1986.
39. Árnadóttir, L.; Stuve, E. M.; Jónsson, H. Adsorption of Water Monomer and Clusters on Platinum(111) Terrace and Related Steps and Kinks II. Surface Diffusion. *Surf. Sci.* **2012**, *606*, 233–238.
40. Nakamura, M.; Ito, M. Coadsorption of Water Dimer and Ring-Hexamer Clusters on M(111) (M = Cu, Ni, Pt) and Ru(001) Surfaces at 25 K as Studied by Infrared Reflection Absorption Spectroscopy. *Chem. Phys. Lett.* **2005**, *404*, 346–350.
41. Ibach, H.; Lehwald, S. The Bonding of Water Molecules to Platinum Surfaces. *Surf. Sci.* **1980**, *91*, 187–197.
42. Jacobi, K.; Bedurftig, K.; Wang, Y.; Ertl, G. From Monomers to Ice—New Vibrational Characteristics of H_2O Adsorbed on Pt(111). *Surf. Sci.* **2001**, *472*, 9–20.
43. Glebov, A. L.; Graham, A. P.; Menzel, A. Vibrational Spectroscopy of Water Molecules on Pt(111) at Submonolayer Coverages. *Surf. Sci.* **1999**, *427−428*, 22–26.
44. Stipe, B. C.; Rezaei, M. A.; Ho, W. Single-Molecule Vibrational Spectroscopy and Microscopy. *Science* **1998**, *280*, 1732–1735.
45. Sainoo, Y.; Kim, Y.; Okawa, T.; Komeda, T.; Shigekawa, H.; Kawai, M. Excitation of Molecular Vibrational Modes with Inelastic Scanning Tunneling Microscopy Processes: Examination through Action Spectra of *cis*-2-Butene on Pd(110). *Phys. Rev. Lett.* **2005**, *95*, 246102.
46. Gawronski, H.; Morgenstern, K.; Rieder, K. H. Electronic Excitation of Ice Monomers on Au(111) by Scanning Tunneling Microscopy—Vibrational Spectra and Induced Processes. *Eur. Phys. J. D* **2005**, *35*, 349–353.
47. Motobayashi, K.; Kim, Y.; Ueba, H.; Kawai, M. Insight into Action Spectroscopy for Single Molecule Motion and Reactions through Inelastic Electron Tunneling. *Phys. Rev. Lett.* **2010**, *105*, 076101.
48. Motobayashi, K.; Katano, S.; Kim, Y.; Kawai, M. Spectral Fitting of Action Spectra for Motions and Reactions of Single Molecules on Metal Surfaces. *Bull. Chem. Soc. Jpn.* **2013**, *86*, 75–79.
49. Motobayashi, K.; Kim, Y.; Arafune, R.; Ohara, M.; Ueba, H.; Kawai, M. Dissociation Pathways of a Single Dimethyl Disulfide on Cu(111): Reaction Induced by Simultaneous Excitation of Two Vibrational Modes. *J. Chem. Phys.* **2014**, *140*, 194705.
50. Michaelides, A.; Ranea, V. A.; de Andres, P. L.; King, D. A. General Model for Water Monomer Adsorption on Close-Packed Transition and Noble Metal Surfaces. *Phys. Rev. Lett.* **2003**, *90*, 216102.
51. Maksymovych, P.; Yates, J. T., Jr. Unexpected Spontaneous Formation of CO Clusters on the Au(111) Surface. *Chem. Phys. Lett.* **2006**, *421*, 473–477.
52. Maksymovych, P.; Sorescu, D. C.; Dougherty, D.; Yates, J. T., Jr. Surface Bonding and Dynamical Behavior of the CH_3SH Molecule on Au(111). *J. Phys. Chem. B* **2005**, *109*, 22463–22468.
53. Rao, B. V.; Kwon, K.-Y.; Liu, A.; Bartels, L. 2,5-Dichlorothiophenol on Cu(111): Initial Adsorption Site and Scanning Tunnel Microscope-Based Abstraction of Hydrogen at High Intramolecular Selectivity. *J. Chem. Phys.* **2003**, *119*, 10879–10884.
54. Ranea, V. A.; Michaelides, A.; Ramírez, R.; de Andres, P. L.; Vergés, J. A.; King, D. A. Water Dimer Diffusion on Pd{111} Assisted by an H-Bond Donor-Acceptor Tunneling Exchange. *Phys. Rev. Lett.* **2004**, *92*, 136104.
55. Ohara, M.; Kim, Y.; Kawai, M. Electric Field Response of a Vibrationally Excited Molecule in an Stm Junction. *Phys. Rev. B: Condens. Matter Mater. Phys.* **2008**, *78*, 201405.
56. Persson, B. N. J.; Baratoff, A. Inelastic Electron Tunneling from a Metal Tip: The Contribution from Resonant Processes. *Phys. Rev. Lett.* **1987**, *59*, 339.
57. Yamamoto, S.; Beniya, A.; Mukai, K.; Yamashita, Y.; Yoshinobu, J. Water Adsorption on Rh(111) at 20 K: From Monomer to Bulk Amorphous Ice. *J. Phys. Chem. B* **2005**, *109*, 5816–5823.
58. Ohara, M.; Kim, Y.; Yanagisawa, S.; Morikawa, Y.; Kawai, M. Role of Molecular Orbitals near the Fermi Level in the Excitation of Vibrational Modes of a Single Molecule at a Scanning Tunneling Microscope Junction. *Phys. Rev. Lett.* **2008**, *100*, 136104.
59. Ueba, H. Analysis of Lateral Hopping of a Single CO Molecule on Pd(110). *Phys. Rev. B: Condens. Matter Mater. Phys.* **2012**, *86*, 035440.
60. Kumagai, T.; Shiotari, A.; Okuyama, H.; Hatta, S.; Aruga, T.; Hamada, I.; Frederiksen, T.; Ueba, H. H-Atom Relay Reactions in Real Space. *Nat. Mater.* **2012**, *11*, 167–172.
61. Kresse, G.; Hafner, J. *Ab Initio* Molecular Dynamics for Liquid Metals. *Phys. Rev. B: Condens. Matter Mater. Phys.* **1993**, *47*, 558–561.
62. Kresse, G.; Hafner, J. Ab Initio Molecular-Dynamics Simulation of the Liquid-Metal-Amorphous-Semiconductor Transition in Germanium. *Phys. Rev. B: Condens. Matter Mater. Phys.* **1994**, *49*, 14251–14269.
63. Kresse, G.; Furthmüller, J. Efficiency of *Ab-Initio* Total Energy Calculations for Metals and Semiconductors Using a Plane-Wave Basis Set. *Comput. Mater. Sci.* **1996**, *6*, 15–50.
64. Kresse, G.; Furthmüller, J. Efficient Iterative Schemes for *Ab Initio* Total-Energy Calculations Using a Plane-Wave Basis Set. *Phys. Rev. B: Condens. Matter Mater. Phys.* **1996**, *54*, 11169–11186.
65. Perdew, J. P.; Wang, Y. Accurate and Simple Analytic Representation of the Electron-Gas Correlation Energy. *Phys. Rev. B: Condens. Matter Mater. Phys.* **1992**, *45*, 13244–13249.
66. Vanderbilt, D. Soft Self-Consistent Pseudopotentials in a Generalized Eigenvalue Formalism. *Phys. Rev. B: Condens. Matter Mater. Phys.* **1990**, *41*, 7892–7895.
67. Kresse, G.; Hafner, J. Norm-Conserving and Ultrasoft Pseudopotentials for First-Row and Transition Elements. *J. Phys.: Condens. Matter* **1994**, *6*, 8245.